sciendo

Int. J. of Applied Mechanics and Engineering, 2022, vol.27, No.3, pp.22-35
DOI: 10.2478/ijame-2022-0033

EVALUATION OF VELOCITY AND ACCELERATION EFFECT ON MECANUM WHEEL ROBOT POSITIONING

Aleksander BĄCZYK*, Przemysław WOJTOWICZ and Tomasz KLEKIEL
University of Zielona Góra, prof. Szafrana 4, Zielona Góra, POLAND
E-mail: a.baczyk@iimb.uz.zgora.pl

In this paper, a Mecanum wheel omnidirectional robotic platform made for taking measurements in harsh and dangerous conditions is introduced. Due to the necessity of highly accurate displacement of the platform for measuring the conditions at the exact measurement point and due to known Mecanum wheel slippage and relatively poor position accuracy, a calibration procedure for minimizing positioning error had to be implemented. For this task, a highly accurate stereographic digital image correlation (DIC) system was used to measure platform displacement. A series of parameters, namely linear maximum velocity and acceleration/deceleration values, were taken into account during the calibration procedure to find the best combination allowing precise movement of the robot. It was found that low acceleration values were the main causes of the robot's poor positioning accuracy and could cause the robot's motors to stall. Max speed values proved to have little effect on the robot's positioning.

Key words: robot, Mecanum wheel, calibration, optical measurements.

1. Introduction

In recent years, an interest in omnidirectional wheels for use in autonomous and remote-controlled robots has increased greatly. Due to specific kinematics, those types of wheels can provide high mobility and *3* degrees of freedom (DOF) for robots without steering axles (Typiak *et al.* [1]). Nowadays, they are widely used in mobile industrial robots and robotic platforms (Hryniewicz *et al.* [2], Guo *et al.* [3]) but they also become used in other mobile robots such as obstacle avoiding robots (Huang *et al.* [4]) and medical equipment (Park *et al.* [5], Hsu *et al.* [6]).

Mecanum wheels, first designed and patented in 1975 by Bengt Erland Ilon [7], are a type of omnidirectional wheels equipped with rollers rotated by *45*° from the wheel axis that acts as a tread. Due to its construction, Mecanum wheels are better suited for heavy loads than standard omni-wheels (Adam *et al.* [8]). However, they have a set of drawbacks, mainly vibrations and poor positioning accuracy due to how their passive rollers make contact with the ground, as was stated by Bae and Kang [9].

To minimize positioning errors of Mecanum wheels, numerous approaches are proposed – both control-sided and purely mechanical. Sun *et al.* [10] employ nonsingular terminal sliding mode to achieve better path following of robotic platform equipped with Mecanum-style wheels while Cao *et al.* [11] prove that fuzzy logic adaptive PID can also reduce the movement error when following a pattern. Chu [12] used multiple ultrasound sensors in dead-reckoning style control of Mecanum wheel robot with correction algorithm. The author also tested the robot's position accuracy with different speeds and how max speed affects the displacement. Qian *et al.* [13] approached the problem differently and applied a suspension mechanism to every wheel of the robotic platform to minimize the wheel vibrations. Bae and Kang [9] experimented with wheel core design, applying flexible roller forks to reduce vibrations and thus positioning errors.

Even though a control-sided and mechanical compensation mechanisms exist and are effective, the positioning problem of Mecanum wheels does not always require complicated solutions and can be corrected by a fundamental mechanism of simply selecting the right acceleration and top speed values in the control

* To whom correspondence should be addressed

scheme. In this paper, the evaluation of the effect of different acceleration values and maximum velocities on the precision of a robotic platform equipped with Mecanum wheels is conducted.

2. Materials and methods

For this evaluation, a four-wheeled robotic platform equipped with four NEMA17 stepper motors was used. Using stepper motors renders using an odometer for wheel rotation measurements obsolete as each step generates a defined and theoretically unchanging linear movement. The step holding option enables the robot to come to a halt when a given number of steps has been reached, reducing the movement that can occur from the robot's inertia. The displacement measurement at given distances was conducted using a high-accuracy digital image correlation system.

2.1. Robotic platform

The robotic platform nicknamed "Uviola", shown in Fig.1, is a four-wheeled vehicle capable of autonomous and remote-controlled driving. It was constructed with a specific task to take measurements in places with high levels of ultraviolet-C (UV-C) radiation which is dangerous to humans. The platform's low profile and low ground clearance was a requirement for neglecting the robot's presence in the test environment so it could reach otherwise unavailable places, e.g. under the table or bed and take measurements.

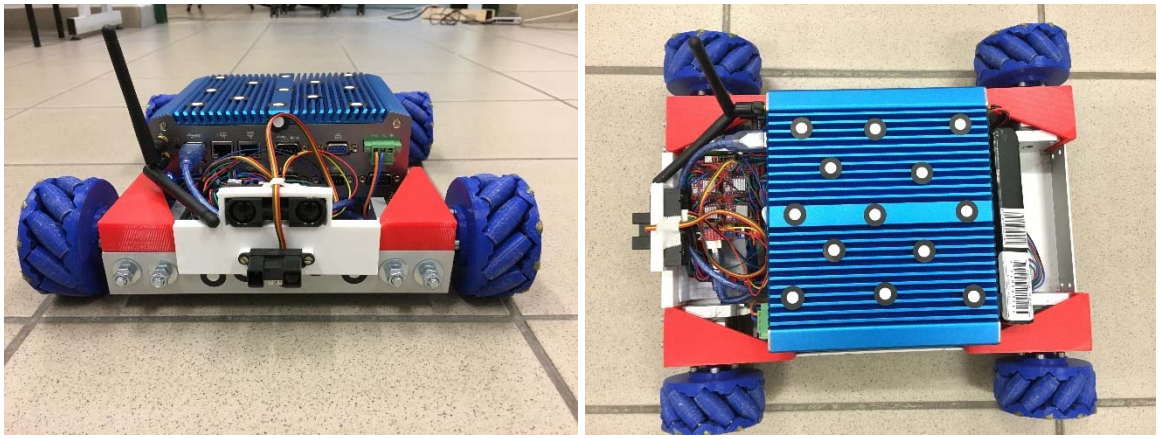

Fig.1. The Uviola robotic platform.

Four 4240 NEMA17 stepper motors with a standard resolution of $200\,steps\,/\,rev$ and a step angle of $1.8°$ are responsible for moving four 3D-printed Mecanum-type wheels consisting of 10 sets of $45°$ rotated rollers each. The motors are controlled individually by four DRV8825 stepper motor drivers (Texas Instruments, USA) working at 4 microstep mode to reduce vibrations at acceleration and deceleration. The master controller was Atmega 328p chip (Microchip Technology Inc., USA) programmed with control firmware responsible for communicating with slave motor drivers and doing distance-to-steps and acceleration/deceleration calculations.

The platform was also equipped with a low-power industrial computer with standard i7 x64 PC architecture (Intel, USA), capable of running desktop Linux or Microsoft Windows operating systems. The main tasks of said computer were to provide an interface for measurement systems carried on the platform and to establish USB-to-UART communication with the Atmega chip to send movement instructions using a designed communication protocol consisting of a series of commands and attributes.

The robot systems were powered by a single rechargeable $11.1V$ lithium-polymer battery rated for $5000\,mAh$ and a discharge current of $50\,C$. The fully charged battery allows 6 hours of continuous operation of the platform.

2.2. Control scheme

The robot has been equipped with two control modes. In mode I, the user could send the exact amount of steps for each stepper motor to be performed in a given direction. This mode was mainly used for calibration and debugging purposes. In mode II, a distance-to-steps (Ξ) calculation was implemented for ease of use. The calculation formula is presented in Eq. 2.1.

$$\Xi = \frac{l}{\xi * \frac{l}{m}}. \tag{2.1}$$

The full step linear distance (ξ) was defined to be the same for both the standard wheel and the Mecanum wheel. The full step linear distance was calculated based on the wheel diameter and resolution of stepper motor (ψ) as given in Eq. 2.2.

$$\xi = \frac{d}{\psi}. \tag{2.2}$$

2.3. Measurement system

The displacement measurements were carried out by ARAMIS dual-camera digital image correlation (DIC) system (Carl Zeiss GOM Metrology GmbH, Germany). The system consists of two Teledyne Dalsa 4M high contrast cameras (Teledyne Technologies Inc., USA) with $24\,mm$ focal length lenses mounted $1.6\,m$ apart and at a $20°$ angle from each other. This setup allows tracking markers displacement over the area of approximately $2\,m^2$. Markers used for tracking platform displacement were $8\,mm$ in diameter. Before the measurements, the system was calibrated by a guided calibration procedure and the measurement error was determined to be $0.0142\,mm$.

2.4. Measurement method

The robotic platform was placed in the field of view of the DIC system as shown in Fig.2.

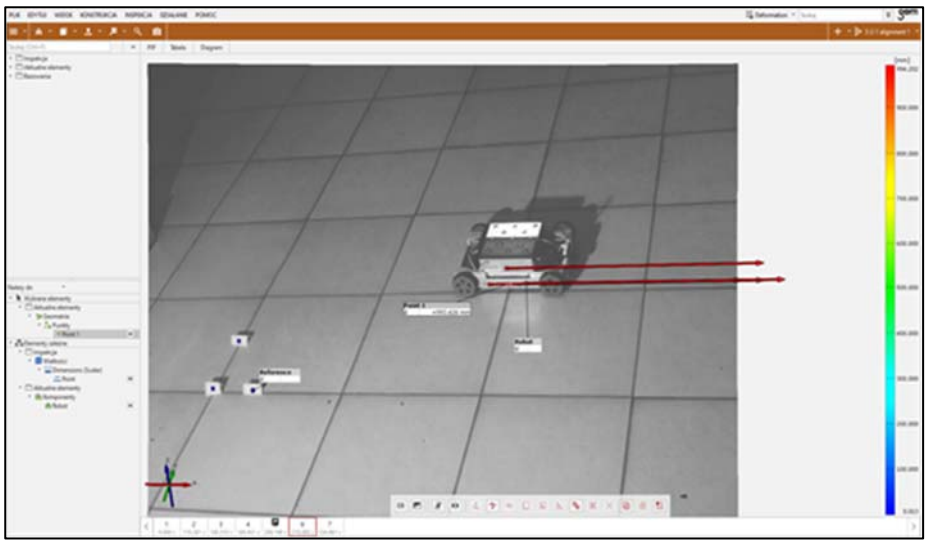

Fig.2. DIC measurements in action with robot visible in camera's FOV.

A series of commands were then sent to the controller to perform movements of the platform: forward / backward $100\,mm$, forward / backward $500\,mm$, and forward / backward $1000\,mm$. The acceleration (a) and max speed (V_{max}) values were changed in each measurement run. The displacement measures were taken at each distance reached by the robot. For reference, a series of measurements were taken using standard $d=75\,mm$ wheels.

3. Results

In the following subsections, the data gathered from the DIC displacement measurements is presented. Measurements of achieved displacement were made for standard and mecanum wheels. Displacement was measured for the following distances: 100, 500, and $1000\,mm$. In this study, three accelerations were compared: 400, 600, and $800\,mm/s^2$ in combination with three top speed values for the standard wheel (50, 100, and $200\,mm/s$) and five for the Mecanum wheel (25, 50, 75, 100, $200\,mm/s$).

3.1. Standard wheels reference

In this subsection, reference measurements for standard wheels with $d=75\,mm$ are presented. Table 1 shows achieved displacement values for given movement distances for the reference standard wheel at the top speed of $50\,mm/s$ and acceleration values of 400, 600 and $800\,mm/s^2$.

Table 1. Measurement of displacement using standard wheels with the maximum speed of $50\,mm/s$.

$[mm]$	$100\,mm$	$-100\,mm$	$500\,mm$	$-500\,mm$	$1000\,mm$	$-1000\,mm$
$400\,mm/s^2$	$98,526$	$98,624$	$507,867$	$508,219$	$993,626$	$994,049$
$600\,mm/s^2$	$98,481$	$98,627$	$496,214$	$496,544$	$993,953$	$994,300$
$800\,mm/s^2$	$98,607$	$98,732$	$496,383$	$496,624$	$994,997$	$994,312$

The targeted distance was not reached in nearly all of the measurements with the exception of the target distance of $500\,mm$ at $400\,mm/s^2$ where an overshoot of $8\,mm \pm 0.2\,mm$ occurred. In other instances, the undershoot of the multiplicity of $2\,mm \pm 0.5\,mm$ occurred regularly. When the acceleration value was set to $800\,mm/s^2$, the difference in targeted and achieved displacement was lowest for all investigated distances. The compared displacement values for the given target distance are presented in Fig.3.

From the plot presented in Fig.3, we can see that the difference in displacement is very similar for all accelerations, except $400\,mm/s^2$ at the distance of $500\,mm$. Table 2 shows achieved displacement values for the standard wheel at $V_{max}=100\,mm/s$.

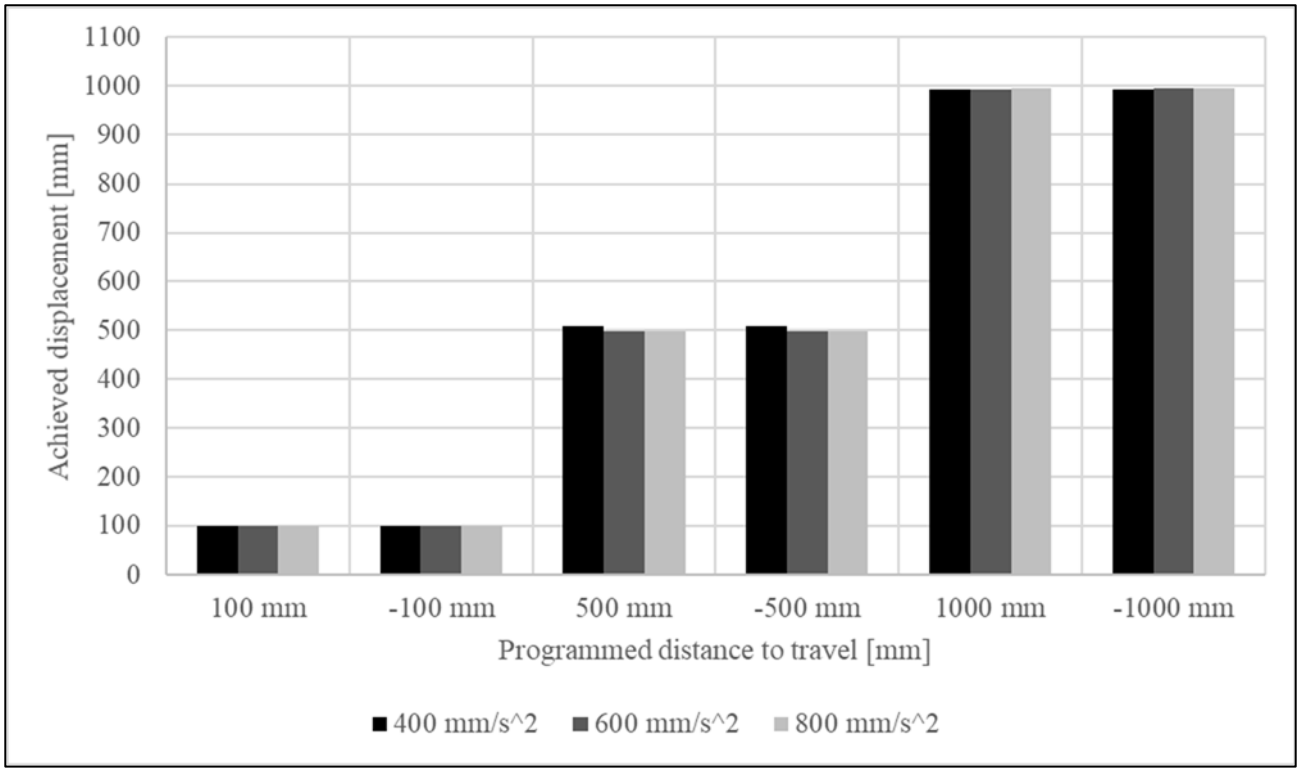

Fig.3. Comparison of displacements for selected accelerations at $V_{max} = 50\,mm/s$ with standard $d = 75\,mm$ wheels.

Table 2. Measurement of displacement using standard wheels with the maximum speed of $100\,mm/s$.

$[mm]$	$100\,mm$	$-100\,mm$	$500\,mm$	$-500\,mm$	$1000\,mm$	$-1000\,mm$
$400\,mm/s^2$	98,761	98,820	495,331	495,736	991,614	992,505
$600\,mm/s^2$	96,787	99,034	497,102	497,541	994,396	994,827
$800\,mm/s^2$	96,917	98,573	495,821	496,200	991,382	991,722

For the distance of $100\,mm$ the lowest error was made with an acceleration value of $400\,mm/s^2$ but only in one direction. With exception of the measurements for forward $100\,mm$, the displacement values closest to the target were achieved for the acceleration of $600\,mm/s^2$. Again, the undershoot value was a multiply of one value, that is $3\,mm \pm 0.3\,mm$. Figure 4 presents compared displacement values for a given target distance.

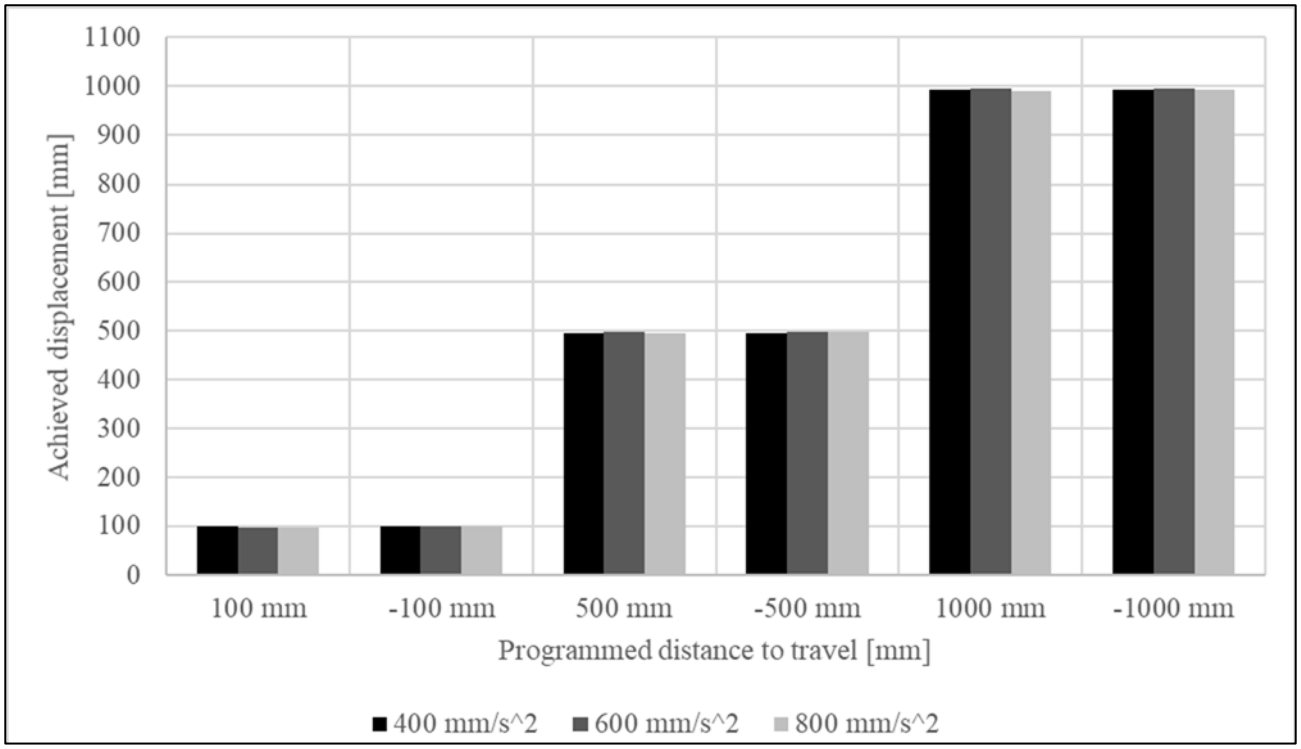

Fig.4. Comparison of displacements for selected accelerations at $V_{max} = 100\,mm/s$ with standard $d = 75\,mm$ wheels.

Only at a targeted distance of $100\,mm$, the displacement error was the lowest for the acceleration of $400\,mm/s^2$. Table 3 contains achieved displacement values for the standard wheel at $V_{max} = 200\,mm/s$.

Table 3. Measurement of displacement using standard wheels with the maximum speed of $200\,mm/s$.

$[mm]$	$100\,mm$	$-100\,mm$	$500\,mm$	$-500\,mm$	$1000\,mm$	$-1000\,mm$
$400\,mm/s^2$	98,395	98,545	495,545	495,992	991,280	992,286
$600\,mm/s^2$	98,455	98,589	495,767	496,241	992,511	992,942
$800\,mm/s^2$	98,667	98,865	497,142	496,894	993,236	993,713

From all of the measurements for set parameters, the lowest difference between targeted and achieved displacement was with acceleration set to $800\,mm/s^2$. At this speed, the undershoot value ranged from $1.5\,mm \pm 0.3\,mm$ at a distance of $100\,mm$ through $4\,mm \pm 1\,mm$ at $500\,mm$ to $7.5\,mm \pm 1.3\,mm$. Figure 5 presents compared displacement values for a given target distance.

On the plot presented in Fig.5, it can be seen that for distances of 500 and $1000\,mm$ the difference in displacement values was the lowest for the acceleration value of $800\,mm/s^2$.

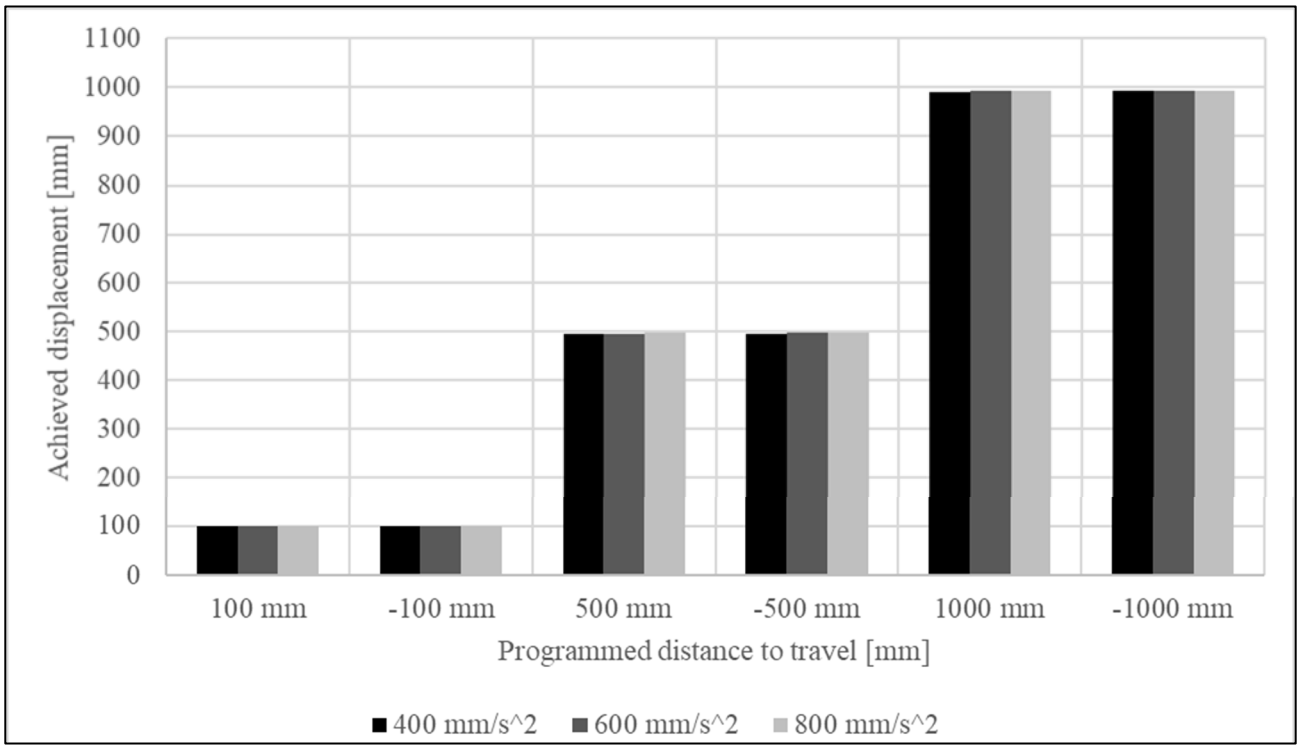

Fig.5. . Comparison of displacements for selected accelerations at $V_{max} = 200\,mm/s$ with standard wheels.

3.2. Mecanum wheels

In this subsection, the measurements conducted with a robot equipped with Mecanum wheels are presented. Table 4 contains displacement measurements at $V_{max} = 25\,mm/s$.

Table 4. Measurement of displacement using Mecanum wheels with the maximum speed of $25\,mm/s$.

$[mm]$	$100\,mm$	$-100\,mm$	$500\,mm$	$-500\,mm$	$1000\,mm$	$-1000\,mm$
$400\,mm/s^2$	$104,996$	$105,364$	$529,943$	$529,284$	$1063,319$	$1061,424$
$600\,mm/s^2$	$105,076$	$103,775$	$531,888$	$528,567$	$1062,368$	$1061,089$
$800\,mm/s^2$	$105,297$	$105,42$	$532,416$	$530,22$	$1065,673$	$1062,094$

With the Mecanum wheels, the positioning error turned positive, overshooting the target value by around $5\,mm \pm 1.3\,mm$ at a target distance of $100\,mm$. At a distance of $500\,mm$, the overshoot value increased around 6 times, being $30\,mm \pm 2,5\,mm$. Another 2 times overshoot increase in regard to the previous measurement was observed at the target distance of $1000\,mm$ giving a total overshoot of $62\,mm \pm 3.6\,mm$. Regarding the target distance, the lowest displacement error occurred with forward movement at $400\,mm/s^2$ However, when going backwards the difference in displacement was lowest for acceleration equal to $600\,mm/s^2$. Figure 6 shows compared displacement values for a given target distance.

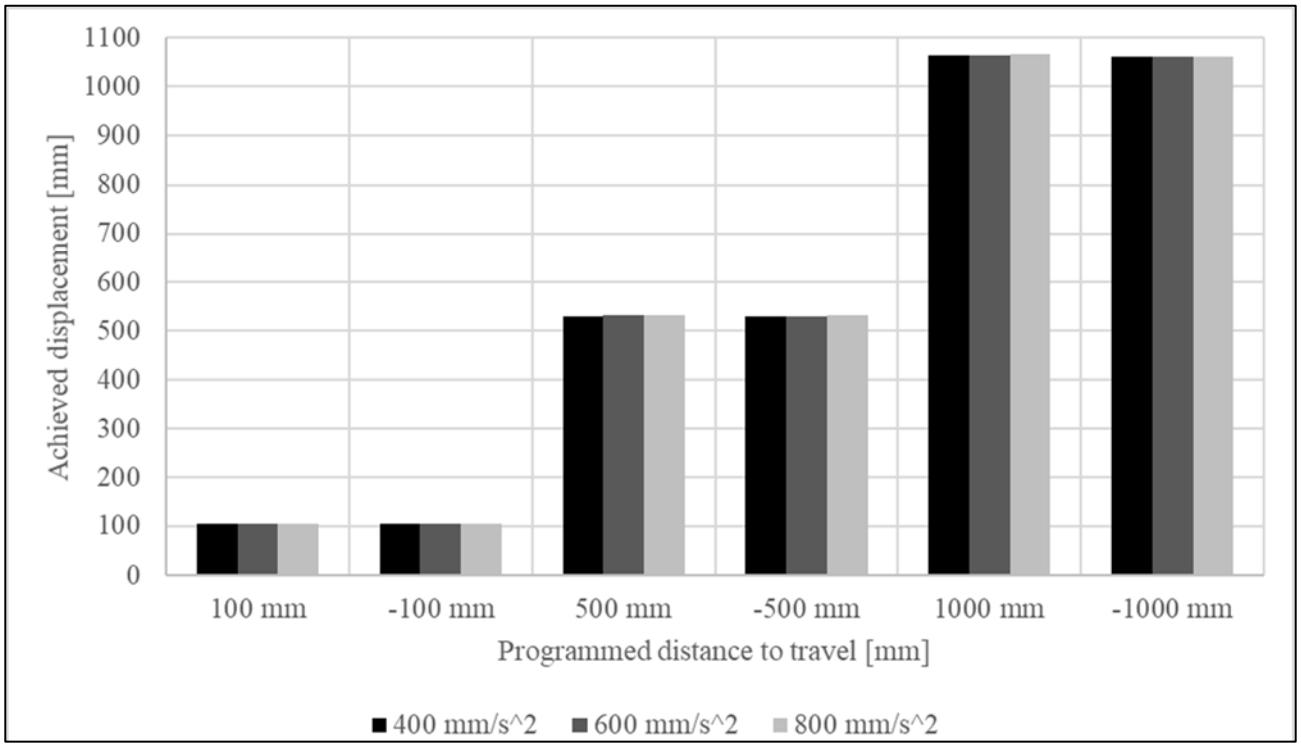

Fig.6. Comparison of displacements for selected accelerations at $V_{max} = 25\,mm/s$ with Mecanum wheels.

An increasing overshoot in the achieved distance is observed as the targeted distance increases. The variation between measured distances at each target distance is between 1.3 to $3.6\,mm$. Table 5 shows achieved displacement values for the standard wheel at $V_{max} = 50\,mm/s$.

Table 5. Measurement of displacement using Mecanum wheels with the maximum speed of $50\,mm/s$.

$[mm]$	$100\,mm$	$-100\,mm$	$500\,mm$	$-500\,mm$	$1000\,mm$	$-1000\,mm$
$400\,mm/s^2$	$99,232$	$105,892$	$527,409$	$532,748$	$1066,687$	$1064,953$
$600\,mm/s^2$	$110,385$	$105,837$	$531,179$	$531,965$	$1065,316$	$1065,341$
$800\,mm/s^2$	$104,047$	$105,109$	$532,663$	$531,348$	$1065,410$	$1064,213$

This time the lowest error in displacement was achieved for a target distance of $100\,mm$ while going forward with an acceleration value of $400\,mm/s^2$. In every other instance, a continuous overshoot is observed. The largest error for the target distance of $100\,mm$ was measured at an acceleration value of $600\,mm/s^2$ while moving forward. Overshoot values were close to previously measured with a bigger overshoot measured at a target distance of $1000\,mm$ at $65\,mm \pm 1.6\,mm$. Figure 7 presents compared displacement values for a given target distance.

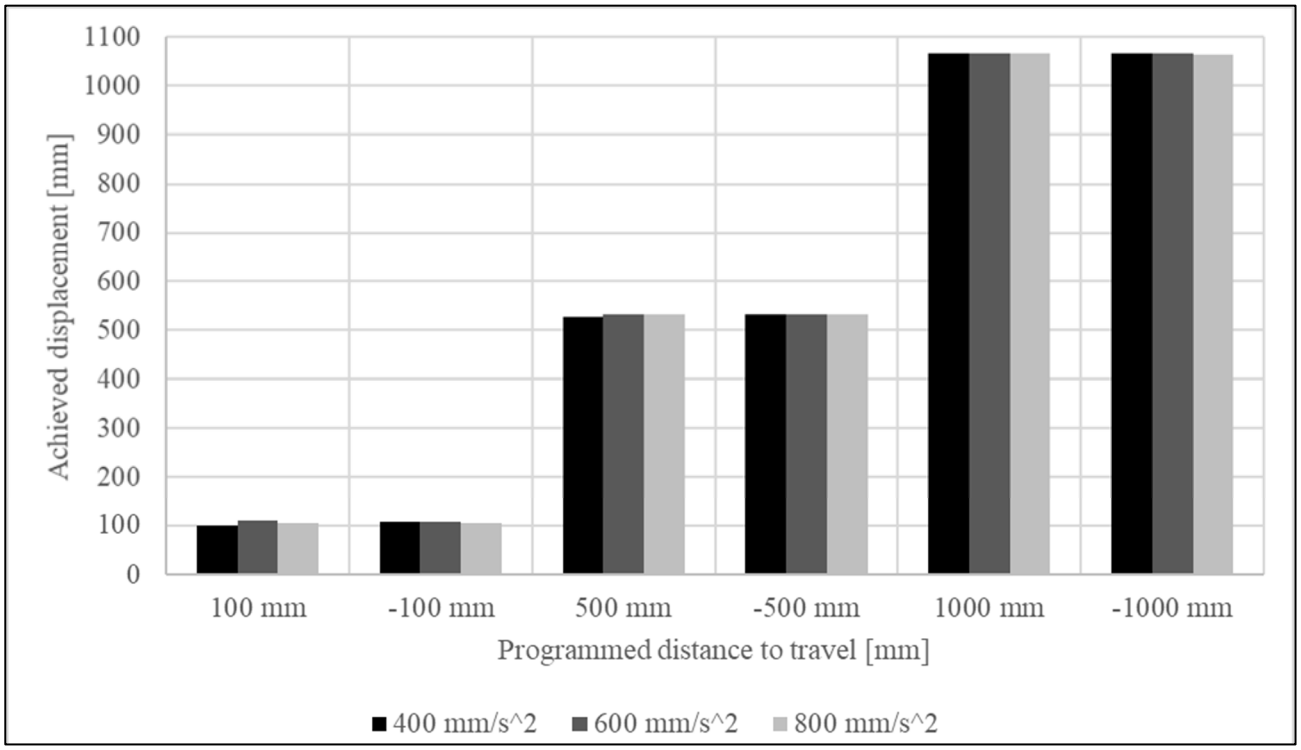

Fig.7. Comparison of displacements for selected accelerations at $V_{max} = 50\,mm/s$ with Mecanum wheels.

Differences in displacement can be seen mainly at target distances of $100\,mm$ and $500\,mm$. Table 6 shows achieved displacement values for the standard wheel at $V_{max} = 75\,mm/s$.

Table 6. Measurement of displacement using Mecanum wheels with the maximum speed of $75\,mm/s$.

$[mm]$	$100\,mm$	$-100\,mm$	$500\,mm$	$-500\,mm$	$1000\,mm$	$-1000\,mm$
$400\,mm/s^2$	105,047	102,360	531,496	529,812	1064,883	1061,439
$600\,mm/s^2$	104,983	103,864	531,511	527,702	1064,621	1061,573
$800\,mm/s^2$	105,420	105,503	533,048	530,980	1066,428	1062,267

At this V_{max}, the lowest overall difference between forward and backward displacement values was measured with an acceleration value equal to $600\,mm/s^2$ with the exception of the $1000\,mm$ distance where the difference was equal to $\pm 3,2\,mm$. The main overshoot values, i.e. $5\,mm$, $30\,mm$, and $60\,mm$, remain the same with ranging variations. Figure 8 shows compared displacement values for a given target distance.

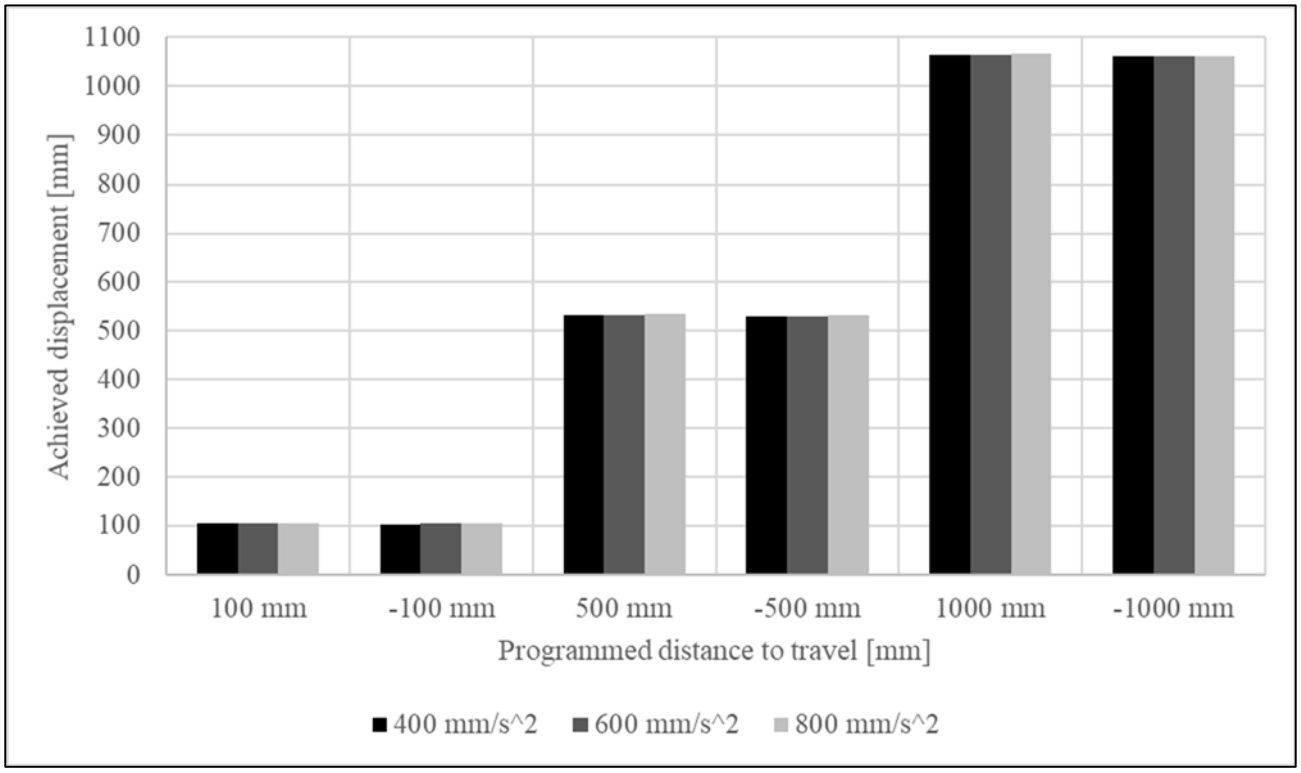

Fig.8. Comparison of displacements for selected accelerations at $V_{max} = 75\,mm/s$ with Mecanum wheels.

From Fig.8 it can be seen that the acceleration value of $600\,mm/s^2$ produced the lowest error in relation to the target value in most of the measurements. Table 7 contains displacement measurements at $V_{max} = 100\,mm/s$.

Table 7. Measurement of displacement using Mecanum wheels with a maximum speed of $100\,mm/s$.

$[mm]$	$100\,mm$	$-100\,mm$	$500\,mm$	$-500\,mm$	$1000\,mm$	$-1000\,mm$
$400\,mm/s^2$	$106,176$	$106,327$	$532,163$	$530,630$	$1067,270$	$1063,182$
$600\,mm/s^2$	$106,123$	$106,265$	$531,886$	$531,135$	$1065,995$	$1064,661$
$800\,mm/s^2$	$106,576$	$106,769$	$532,769$	$531,534$	$1066,786$	$1064,196$

With set V_{max}, the position accuracy while neglecting the overshoot at the target distance of $100\,mm$ varies around $\pm 0.2\,mm$ for every tested acceleration value. At the distance of $500\,mm$ and $1000\,mm$, the lowest difference between achieved displacements can be observed for the acceleration of $600\,mm/s^2$ with positioning error of $\pm 0.7\,mm$ at $500\,mm$ and $\pm 1.3\,mm$ at $1000\,mm$. The overall overshoot distances remain nearly the same as for the previous measurements. Figure 9 presents compared displacement values for a given target distance.

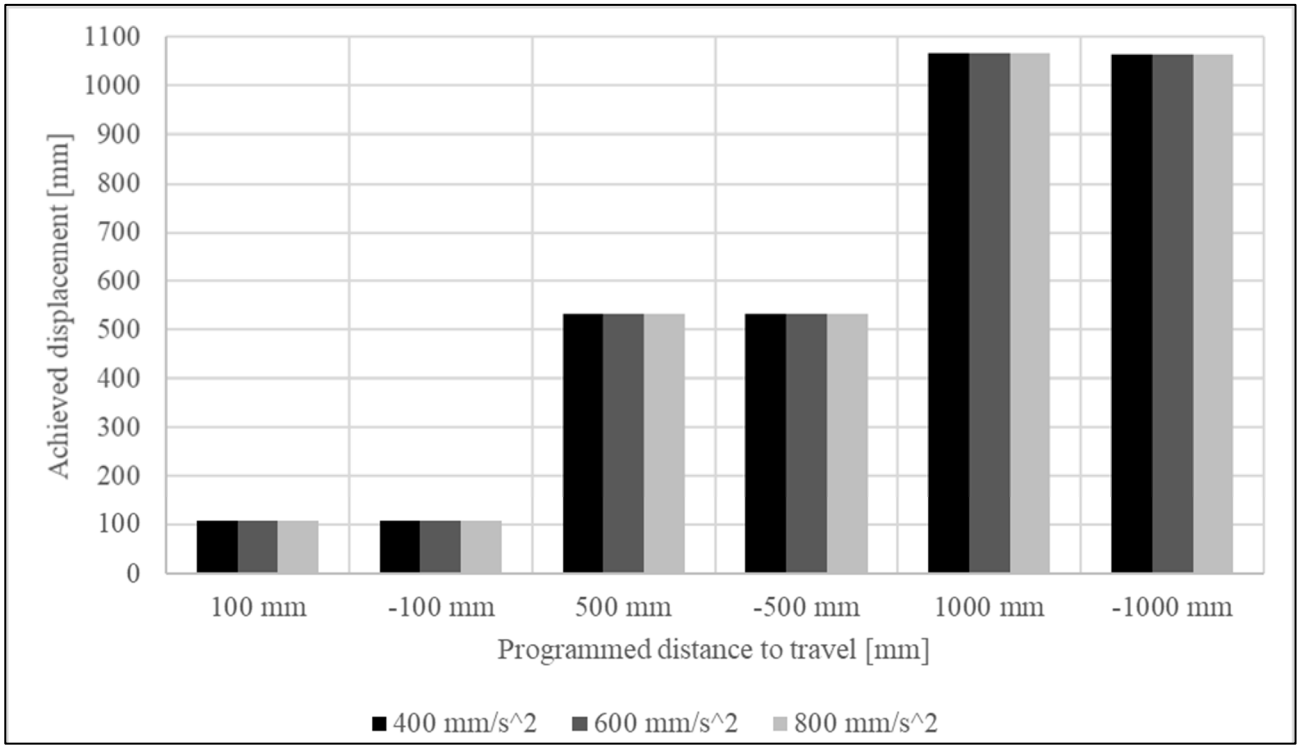

Fig.9. Comparison of displacements for selected accelerations at $V_{max} = 100\,mm/s$ with Mecanum wheels.

The highest differences in achieved displacements can be seen for a target distance of $1000\,mm$. Table 8 contains displacement measurements at $V_{max} = 200\,mm/s$.

Table 8. Measurement of displacement using Mecanum wheels with the maximum speed of $200\,mm/s$.

$[mm]$	$100\,mm$	$-100\,mm$	$500\,mm$	$-500\,mm$	$1000\,mm$	$-1000\,mm$
$400\,mm/s^2$	105,907	106,289	532,344	530,301	1067,096	1064,573
$600\,mm/s^2$	106,946	106,629	532,525	531,667	1064,575	1065,000
$800\,mm/s^2$	106,004	106,224	531,655	531,787	1065,458	1065,720

At set velocity, the lowest difference between forward and backward movement at a target distance of $100\,mm$ and $500\,mm$ was observed for acceleration value of $800\,mm/s^2$ at $\pm 0.2\,mm$ and $\pm 0.3\,mm$ at a target distance of $1000\,mm$. Biggest differences could be observed at $500\,mm$ and $1000\,mm$ distance for $400\,mm/s^2$ and $600\,mm/s^2$ going as high as $\pm 2\,mm$ for $a=400\,mm/s^2$. Again, the overall overshoot distances remained the same. Figure 10 presents compared displacement values for a given target distance.

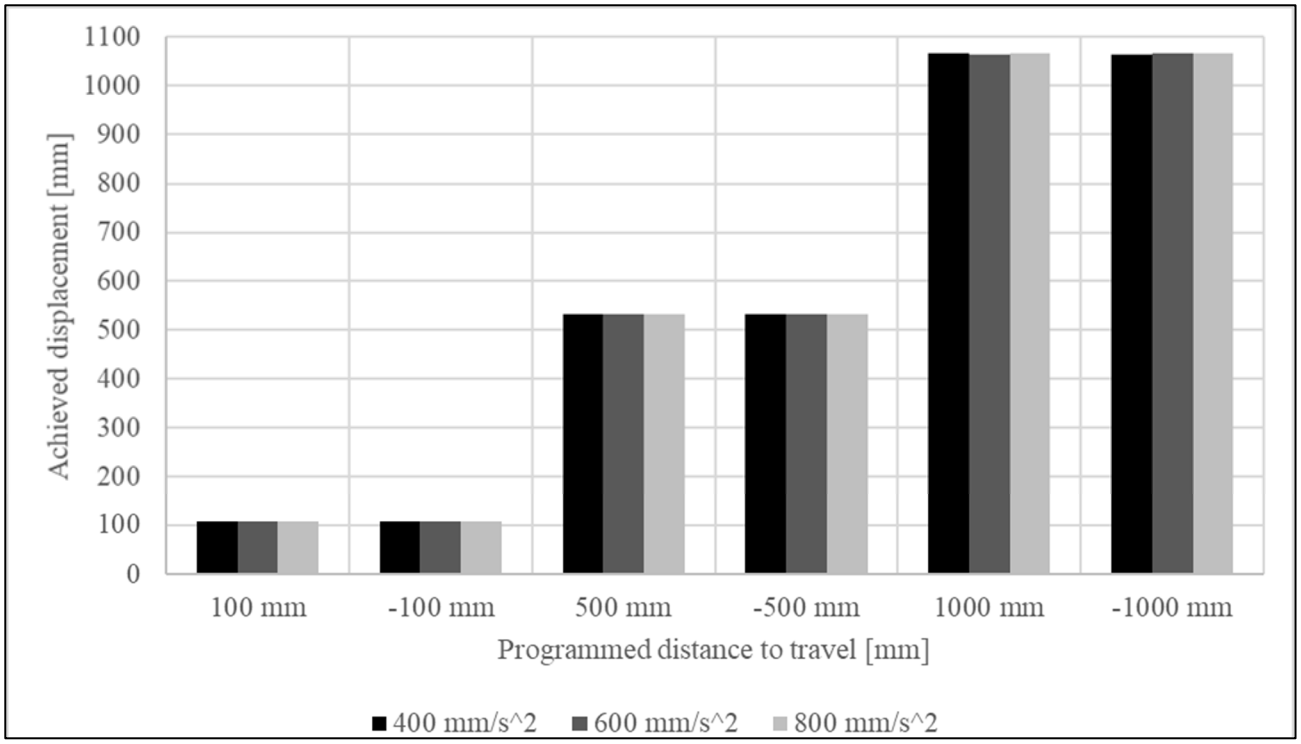

Fig.10. Comparison of displacements for selected accelerations at $V_{max}=200\,mm/s$ with Mecanum wheels.

The biggest difference in displacement can be seen at a target distance of $500\,mm$ and $1000\,mm$ for acceleration $400\,mm/s^2$.

4. Conclusion

The robotic systems displacement calibration process is essential for achieving precise positioning of the machine. Simple calculations based on the wheel diameter will not always be precise enough and could result in recurring positioning error. Top velocity and acceleration value also play a significant role in precise positioning.

Analyzing the data acquired from the DIC measurements it becomes clear that the lower speed and acceleration, the more unforeseeable displacement occurs. This statement is especially true for Mecanum wheels, where it is apparent that the wheel requires a certain velocity and acceleration to reach said velocity to move with recurring precision. It is also notable that during tests with accelerations lower than $400\ mm/s^2$, the stepper motors would stall on an irregular basis.

Undershoot observed on standard wheels and overshoot observed on Mecanum wheels could be caused by chosen ξ parameter. Since the under and overshooting occurred with a certain scheme, a simple correction parameter can be implemented and with known displacement measurements it could minimize the under and overshooting. It is also worth mentioning that simple distance sensors, like ultrasound or laser ones can

increase the positioning accuracy by providing feedback to the control system, given a suitable reference point, i.e. wall or another obstacle, is found and the sensor provides adequately precise output.

Acknowledgments

This article was prepared and published in the scope of the project: *The use of UV-C technology to reduce the transmission of SARS-CoV-2 virus and limit the transmission of infections in hospitals*, numbered: $SZPITALE - JEDNOIMIENNE/57/2020$ and financed by the Polish National Centre for Research and Development (NCBiR)

Nomenclature

Ξ – amount of steps based on distance
l – linear distance mm
ξ – full step linear distance mm
m – microstepping multipler
d – diameter mm
ψ – stepper motor resolution
V – velocity mm/s
V_{max} – maximum velocity mm/s
a – acceleration mm/s^2

References

[1] Typiak A., Łopatka M. J., Rykała Ł. and Kijek M. (2018): *Dynamics of omnidirectional unmanned rescue vehicle with mecanum wheels.*– AIP Conference Proceedings 1922, Article No.120005, p.10, https://doi.org/10.1063/1.5019120.

[2] Hryniewicz P., Gwiazda A., Banaś W., Sękala A. and Foit K. (2017): *Modelling of a mecanum wheel taking into account the geometry of road rollers.*– IOP Conference Series: Materials Science and Engineering, vol.227, Article No.012060.

[3] Guo S., Shuai Q. and Xi F. (2017). *Vision based navigation for omni-directional mobile industrial robot*.– Procedia Computer Science, vol.105, pp.20-26.

[4] Huang Y., Meng R., Yu J., Zhao Z. and Zhang X. (2022): *Practical obstacle-overcoming robot with a heterogeneous sensing system: design and experiments*.– Machines, vol.10, Article No.289, https://doi.org/10.3390/machines10050289.

[5] Park J., An B., Kwon O. and Yi H. (2022): *User intention based intuitive mobile platform control: application to a patient transfer robot*.– Int. J. Precis. Eng. Manuf., vol23, pp.653-666.

[6] Hsu P. E., Hsu Y. L., Chang K. W., and Geiser C. (2012): *Mobility assistance design of the intelligent robotic wheelchair.*– International Journal of Advanced Robotic Systems, vol.9, No.6, p.10, https://doi.org/10.5772/54819.

[7] Ilon B. E. (1975): *Wheels for a course stable selfpropelling vehicle movable in any desired direction on the ground or some other base.*– US Patent No.3,876,255.

[8] Adam N., Aiman M., Nafis W.M., Irawan A., Muaz M., Hafiz M. and Sheikh Ali S.N. (2016): *Omnidirectional configuration and control approach on mini heavy loaded forklift autonomous guided vehicle.*– MATEC Web of Conferences, vol.90, Article No.01077, p.11, https://doi.org/10.1051/matecconf/20179001077.

[9] Bae J.-J. and Kang N. (2016): *Design optimization of a mecanum wheel to reduce vertical vibrations by the consideration of equivalent stiffness.*– Shock and Vibration, vol.2016, Article No.5892784, p.8, https://doi.org/10.1155/2016/5892784.

[10] Sun Z., Xie H., Zheng J., Man Z., and He D. (2021): *Path-following control of mecanum-wheels omnidirectional mobile robots using nonsingular terminal sliding mode.*– Mechanical Systems and Signal Processing, vol.147, Article No.107128, p.14, https://doi.org/10.1016/j.ymssp.2020.107128.

[11] Cao G., Zhao X., Ye C. and Yu S. (2022): *Fuzzy adaptive PID control method for multi-mecanum-wheeled mobile robot.*– J. Mech. Sci. Technol., vol.36, pp.2019-2029, DOI:10.1007/s12206-022-0337-x.

[12] Chu B. (2017): *Position compensation algorithm for omnidirectional mobile robots and its experimental evaluation.*– International Journal of Precision Engineering and Manufacturing, vol.18, No.12, pp.1755-1762.

[13] Qian J., Zi B., Wang D., Ma Y. and Zhang D. (2017): *The design and development of an omni-directional mobile robot oriented to an intelligent manufacturing system.*– Sensors, vol.17, No.9, Article No.2073, p.15, https://doi.org/10.3390/s17092073.

Received: June 6, 2022
Revised: August 15, 2022